Nanomedicines

Deutsche Ausgabe: DOI: 10.1002/ange.201602525
Internationale Ausgabe: DOI: 10.1002/anie.201602525

Bilirubin Nanoparticles as a Nanomedicine for Anti-inflammation Therapy

*Yonghyun Lee, Hyungjun Kim, Sukmo Kang, Jinju Lee, Jinho Park, and Sangyong Jon**

Abstract: *Despite the high potency of bilirubin as an endogenous anti-inflammatory compound, its clinical translation has been hampered because of its insolubility in water. Bilirubin-based nanoparticles that may overcome this critical issue are presented. A polyethylene glycol compound (PEG) was covalently attached to bilirubin, yielding PEGylated bilirubin (PEG-BR). The PEG-BR self-assembled into nanoscale particles with a size of approximately 110 nm, termed bilirubin nanoparticles (BRNPs). BRNPs are highly efficient hydrogen peroxide scavengers, thereby protecting cells from H_2O_2-induced cytotoxicity. In a murine model of ulcerative colitis, intravenous injection of BRNPs showed preferential accumulation of nanoparticles at the sites of inflammation and significantly inhibited the progression of acute inflammation in the colon. Taken together, BRNPs show potential for use as a therapeutic nanomedicine in various inflammatory diseases.*

Bilirubin, a yellow bile pigment that comprises the final metabolite of the heme catabolic pathway, is a potent endogenous antioxidant capable of scavenging various reactive oxygen species (ROS), thereby playing a crucial role in protecting cells, and the body as a whole, from oxidative stress-mediated damage.[1] To date, a number of studies have investigated the physiological role of bilirubin in our body, and its potential uses as a medicine. Indeed, a recent epidemiological study indicates that individuals with higher levels of total serum bilirubin experience various health benefits, including a lower risk of certain cardiovascular diseases and cancers.[2] Moreover, the therapeutic efficacy of bilirubin has been demonstrated and confirmed by many scientists in various experimental animal models of inflammatory diseases, ranging from acute to chronic inflammation.[3] All such previous studies have clearly revealed that bilirubin is a highly potent anti-inflammatory and anticancer compound in our body.

However, because of its insolubility in water, bilirubin can only be administered by intraperitoneal injection,[3] which is a highly unfavorable route of administration for treating patients. Additionally, the free bilirubin injected externally may become deposited in various tissues, thereby causing a jaundice signature and resulting in potential toxicity.[4] As a result, despite its obvious potential health benefits, the clinical usage of bilirubin has been limited.

To date, bilirubin-based nanomaterials have not been developed and utilized for biomedical applications. Here, we provide the first report on bilirubin-based nanoparticles (BRNPs) and their use as a therapeutic nanomedicine for inflammatory diseases.[5] Owing to the powerful ability of bilirubin to scavenge various ROS and modulate the immune system,[3c,e,6] BRNPs also exerted a potent, intrinsic therapeutic effect, as evidenced by their high efficacy in an animal model of acute inflammatory diseases.

To address the insolubility of bilirubin in its natural form, polyethylene glycol (PEG; molecular weight, 2000 g mol^{-1}) was covalently attached to this compound by a stable amide bond (Figure 1a), and the resulting PEGylated bilirubin (PEG-BR) was characterized by proton nuclear magnetic resonance, mass spectrometry, elemental analysis, and infrared (IR) and ultraviolet-visible (UV/Vis) spectrophotometry analyses (Supporting Information, Figures S1 and S2).

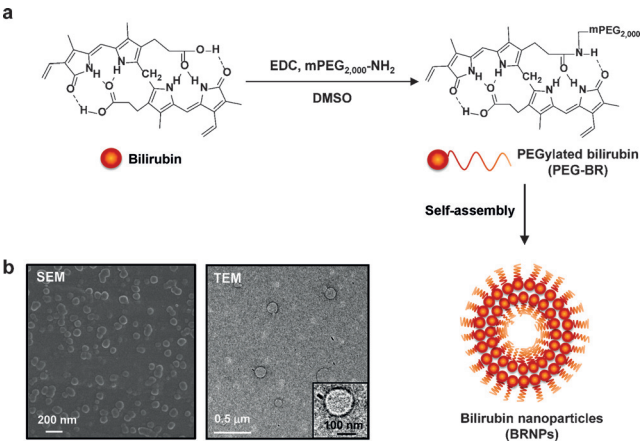

Figure 1. Bilirubin nanoparticles (BRNPs) are formed from PEGylated bilirubin (polyethylene glycol (PEG)-BR). a) Synthesis of PEG-BR starting from free bilirubin and free PEG, and the formation of BRNPs self-assembled from PEG-BRs in PBS. b) SEM and TEM images of BRNPs.

We hypothesized that, as an amphiphile, PEG-BR would self-assemble into a nanostructure because of interactions among individual hydrophobic bilirubin molecules. Dynamic light-scattering (DLS) measurements revealed that PEG-BR formed nanoscale particles with a hydrodynamic size of 136 ± 9 nm at concentrations greater than about 10 nM, and that the size of the nanoparticles remained unchanged after

[*] Dr. Y. Lee, Dr. H. Kim, S. Kang, Dr. J. Lee, Dr. J. Park, Prof. Dr. S. Jon
KAIST Institute for the BioCentury,
Department of Biological Sciences,
Korea Advanced Institute of Science and Technology (KAIST)
291 Daehak-ro, Daejeon 34141, (Republic of Korea)
E-mail: syjon@kaist.ac.kr

Supporting information for this article can be found under: http://dx.doi.org/10.1002/anie.201602525.

© 2016 Wiley-VCH Verlag GmbH & Co. KGaA, Weinheim

8 days of incubation (Supporting Information, Figure S3). As shown in the scanning electron microscopy (SEM) and transmission electron microscopy (TEM) images presented in Figure 1b, the size of the BRNPs in the air-dried state was 94 ± 13 nm (data are presented as mean ± standard deviation (s.d.); $n = 104$ particles in the SEM image). The magnified TEM image of a representative BRNP is shown in the inset of Figure 1b. Although a similar PEGylated bilirubin compound was previously produced to study the pK_a value of the bilirubin derivative,[7] no suggestions or implications regarding the potential biomedical applications of the compound were made in that study.

Previous studies have shown that ROS are involved in the progression and pathogenesis of various acute and chronic inflammatory diseases.[8] As such, we first examined whether BRNPs could scavenge ROS, and thereby protect cells from oxidative damage. Addition of BRNPs to an aqueous solution of H_2O_2 (50 μM) resulted in a significant reduction in the concentration of hydrogen peroxide, an effect that was BRNP concentration dependent (Figure 2a). Moreover, BRNPs effectively protected cells from H_2O_2-induced cytotoxicity (Figure 2b; Supporting Information, Figure S5), indicating the ROS-scavenging power of these nanoparticles.

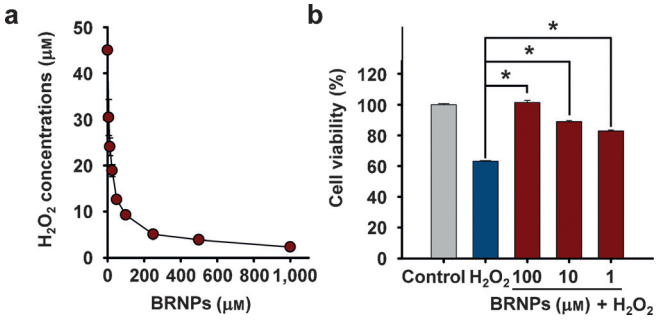

Figure 2. BRNPs exert a cytoprotective effect by scavenging reactive oxygen species (ROS). a) Concentration of H_2O_2 remaining after treatment of BRNPs with H_2O_2 (50 μM) for 40 min, as quantified by measuring fluorescence intensity using a horseradish peroxidase/dye reagent. Data are presented as the mean ± standard error of the mean (s.e.m.; $n = 6$). b) Viability of CHO-K1 cells treated with culture medium, H_2O_2 (500 μM), or H_2O_2 (500 μM) and BRNPs (100, 10, or 1 μM) for 8 h. Data are presented as the mean ± s.e.m. ($n = 6$; *$P < 0.001$, one-way analysis of variance (ANOVA)).

Subsequently, we evaluated the therapeutic efficacy of BRNPs in an acute inflammation model. We hypothesized that BRNPs would 1) circulate longer in the blood owing to their PEGylated surfaces, 2) preferentially accumulate at sites of inflammation where vascular structures are leaky owing to active, pathological angiogenesis,[9] and 3) exhibit therapeutic efficacy within the inflammatory site because of their intrinsic ability to effectively scavenge ROS and modulate the immune system.[3a,c,e,6] To test these hypotheses, we induced intestinal inflammation in female C57BL/6 mice by supplying them with a 3% solution of dextran sodium sulfate (DSS) instead of drinking water for 5 days,[10] The mice were then intravenously administered with indocyanine green (ICG)-loaded BRNPs (ICG@BRNPs; Figure 3a). While bioimaging

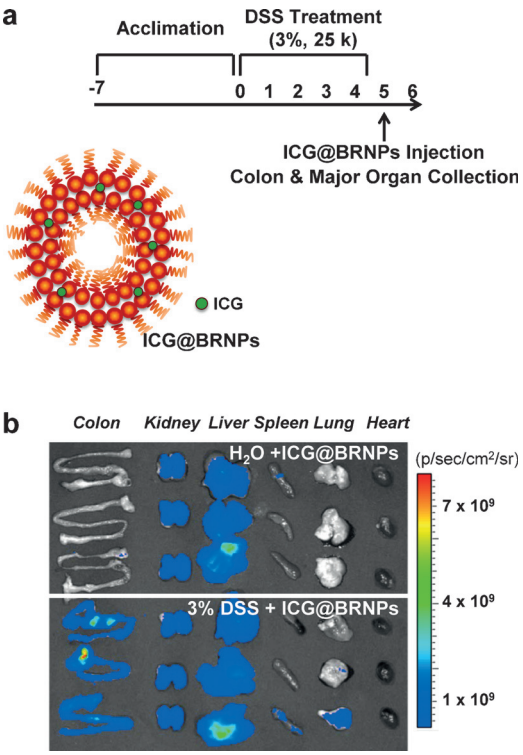

Figure 3. BRNPs can be preferentially localized in an inflamed colon. a) The overall experimental procedure. Mice were provided with normal water (H_2O) or water containing 3% DSS for 5 days. On day 5, the mice were intravenously injected with indocyanine green (ICG)-loaded BRNPs (ICG@BRNPs). b) Biodistribution images in the organs of mice treated with ICG@BRNPs (17 μg ICG; 340 μg BRNPs) were taken at 5 h post injection.

revealed little fluorescence in the colons of normal mice ($n = 3$), strong signals were detected in the colons of colitis mice ($n = 3$), indicating that ICG@BRNPs preferentially localized at the site of inflammation (Figure 3b). We speculate that the preferential localization of ICG@BRNPs was mediated by increased vascular permeability in the inflammatory colon.[9]

Encouraged by these inflammation-targeting results, we evaluated the therapeutic efficacy of BRNPs in the colitis model. For these analyses, a single intravenous injection of either BRNPs ($125\ mg\,kg^{-1}$) or phosphate-buffered saline (PBS; control) was administered on day 1 during preparation of the colitis model, and therapeutic efficacy was assessed on day 9 (Figure 4a). Colitis model mice treated with PBS exhibited a significant loss of body weight. Conversely, the body weight of mice in the BRNP-treated group was similar to that in the normal control group (Figure 4b). Colon length is an important parameter for assessing treatment efficacy in the colitis model.[10] Unlike the colons of the normal mice, those of the colitis model mice were significantly shorter and there were signs of bleeding indicative of severe inflammation (Figure 4c). These mice also exhibited loose stools or diarrhea (data not shown). In contrast, the colitis model mice treated with a single injection of BRNPs showed little evidence of bleeding, colon shortening, or abnormal stools. Histological analyses of hematoxylin and eosin (H&E)

 © 2016 Wiley-VCH Verlag GmbH & Co. KGaA, Weinheim

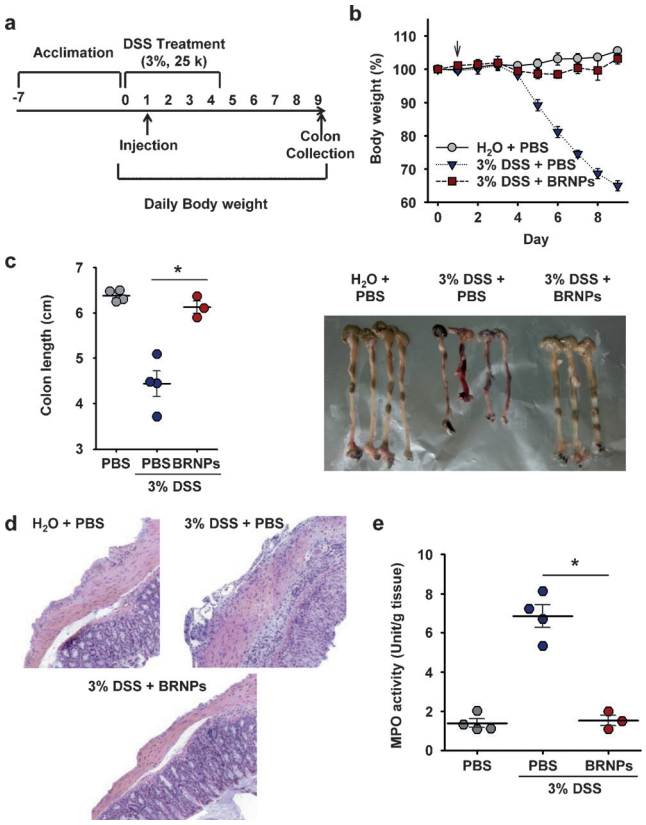

Figure 4. BRNPs show remarkable anti-inflammatory effects in a murine dextran sodium sulfate (DSS)-induced colitis model. a) The overall experimental procedure. Mice were provided with normal water (H_2O) or water containing 3% DSS for 5 days. On day 1, the mice were intravenously injected with BRNPs (125 mg kg^{-1}) or phosphate buffered saline (PBS). b) Daily body weight change in the mice in each group over 9 days. Data are presented as the mean ± s.e.m ($n = 3$–4). c) Mice were sacrificed on day 9, and colons were harvested, imaged, and their lengths compared. Data are presented as the mean ± s.e.m. ($n = 3$–4; *$P < 0.05$, Kruskal–Wallis test). d) Hematoxylin and eosin (H&E) stained colon sections from each group of mice on day 9. e) Colonic myeloperoxidase (MPO) activity. MPO assays were performed on colonic tissues. Data are presented as the mean ± s.e.m. ($n = 3$–4; *$P < 0.05$, Kruskal–Wallis test).

stained colon sections further revealed only minor damage to the mucosal areas of the colons and little infiltration of immune cells in the mucosa, submucosa, or muscle/serosa of mice treated with BRNPs. In contrast, severe destruction of mucosal areas, colonic epithelial damage, and massive infiltration of immune cells was observed in the samples from the colitis mice treated with PBS (Figure 2d); these effects were subsequently quantified using a colon damage scoring system (Supporting Information, Figure S5a).[10b] Subsequently, we measured the activity of myeloperoxidase (MPO), which is closely correlated with inflammatory bowel disease (IBD) severity,[10a] in colon samples harvested from control and colitis model mice. While MPO activity was highly elevated in the colons of the mice in the colitis group compared to those in the normal group, activity was dramatically decreased in the colons of mice in the BRNP-treated group (Figure 4e). In experimental colitis, disease severity is also often correlated with increased levels of proinflammatory cytokines.[10a] Notably, there were significantly lower levels of the proinflammatory cytokines interleukin (IL)-1, IL-6, tumor necrosis factor (TNF)-α, and interferon (IFN)-γ within the colonic tissues of mice treated with BRNPs compared to those in the PBS-treated group (Supporting Information, Figure S5b). Collectively, these data clearly indicate that our BRNPs are highly effective inhibitors of the pathogenesis and/or progression of acute colitis, and therefore show potential as a therapeutic option for treatment of various inflammatory diseases.

Finally, we performed single-dose toxicity tests to examine the toxicity of BRNPs both in vitro and in vivo. Even at the highest concentration tested (100 μM), BRNPs had no effect on the viability of CHO-K1 cells after 8 h treatment (Figure 5a). For in vivo tests, mice were intravenously injected

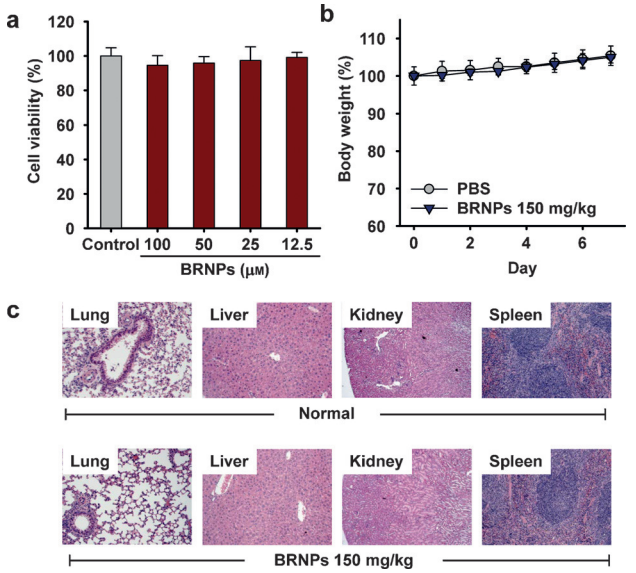

Figure 5. BRNPs are well-tolerated both in vitro and in vivo. a) Viability of CHO-K1 cells treated with different concentrations of BRNPs for 8 h. Data are presented as the mean ± s.e.m. ($n = 12$). b) Daily body weight change in mice treated with BRNPs (150 mg kg^{-1}) or phosphate buffered saline (PBS) by intravenous injection. Data are presented as the mean ± s.e.m. ($n = 6$). c) Representative images of hematoxylin and eosin (H&E) stained sections of indicated organs harvested from mice at one week after intravenous administration of BRNPs (150 mg kg^{-1}) or PBS.

with 150 mg kg^{-1} BRNPs; this dose is equivalent to approximately 581 mg bilirubin per liter of blood volume (58.5 mL blood kg^{-1} body weight in mice), which is approximately 58-fold higher than the normal total concentration of serum bilirubin (ca. 3–12 mg L^{-1}).[11] At this dose, BRNPs had little apparent toxicity, as evidenced by a lack of major behavior changes or weight loss (Figure 5b), and unchanged blood test parameters (Supporting Information, Figure S6) such as liver function values and results from hematological analyses. There was also no histological evidence of damage to major organs (Figure 5c). The bilirubin in BRNPs is covalently linked to hydrophilic PEG by a stable amide bond, consequently there was little concern that it would be

© 2016 Wiley-VCH Verlag GmbH & Co. KGaA, Weinheim

deposited in the skin or the sclera of the eye. As expected, no visibly detectable signs of yellowing in the skin or eyes were observed in the mice examined (data not shown). These toxicity tests suggest that BRNPs comprised of PEGylated bilirubin are safe and sufficiently biocompatible for potential use in clinical applications.

In conclusion, for the first time a nanomaterial comprised of an endogenous bioactive compound, bilirubin (bilirubin nanoparticles; BRNPs), has been developed and applied in a biomedical setting as an anti-inflammatory therapeutic agent. In an animal model similar to IBD (that is, without the aid of therapeutic drugs), BRNPs exerted potent anti-inflammatory effects, presumably owing to the ability of bilirubin to scavenge a variety of ROS and modulate the immune responses. We also found that BRNPs show highly potent therapeutic efficacy in animal models of acute asthma and hepatic ischemic reperfusion injury (data not shown), results that will be published separately. Notably, these beneficial effects were associated with little or no toxicity. The potential application of this material is made more feasible by the fact that BRNPs are composed of clinically approved PEG and bilirubin, an endogenous antioxidant bile pigment. Together, our findings breathe new life into the potential clinical applications of bilirubin: by simple introduction of PEG, the resulting BRNPs pave the way to the next generation of novel therapeutics for oxidative stress-associated diseases ranging from acute to chronic diseases.

Acknowledgements

This work was supported by a Global Research Laboratory grant (2015045887) and the KAIST Future Systems Healthcare Project through the National Research Foundation of Korea (NRF), funded by the Ministry of Science, ICT & Future Planning.

Keywords: bilirubin · inflammation therapy · nanomedicine · nanoparticles · self-assembled nanostructures

How to cite: *Angew. Chem. Int. Ed.* **2016**, *55*, 7460–7463
Angew. Chem. **2016**, *128*, 7586–7589

[1] a) R. Stocker, Y. Yamamoto, A. F. McDonagh, A. N. Glazer, B. N. Ames, *Science* **1987**, *235*, 1043–1046; b) S. Dore, M. Takahashi, C. D. Ferris, R. Zakhary, L. D. Hester, D. Guastella, S. H. Snyder, *Proc. Natl. Acad. Sci. USA* **1999**, *96*, 2445–2450; c) D. E. Baranano, M. Rao, C. D. Ferris, S. H. Snyder, *Proc. Natl. Acad. Sci. USA* **2002**, *99*, 16093–16098; d) T. W. Sedlak, M. Saleh, D. S. Higginson, B. D. Paul, K. R. Juluri, S. H. Snyder, *Proc. Natl. Acad. Sci. USA* **2009**, *106*, 5171–5176.

[2] a) L. J. Horsfall, G. Rait, K. Walters, D. M. Swallow, S. P. Pereira, I. Nazareth, I. Petersen, *JAMA J. Am. Med. Assoc.* **2011**, *305*, 691–697; b) H. A. Schwertner, L. Vitek, *Atherosclerosis* **2008**, *198*, 1–11; c) S. D. Zucker, P. S. Horn, K. E. Sherman, *Hepatology* **2004**, *40*, 827–835.

[3] a) S. D. Zucker, M. E. Vogel, T. L. Kindel, D. L. Smith, G. Idelman, U. Avissar, G. Kakarlapudi, M. E. Masnovi, *Am. J. Physiol. Gastrointest. Liver Physiol.* **2015**, 00149–02014; b) R. Ben-Amotz, J. Bonagura, M. Velayutham, R. Hamlin, P. Burns, C. Adin, *Front. Physiol.* **2014**, *5*, 53; c) Y. Liu, P. Li, J. Lu, W. Xiong, J. Oger, W. Tetzlaff, M. Cynader, *J. Immunol.* **2008**, *181*, 1887–1897; d) R. Ollinger, M. Bilban, A. Erat, A. Froio, J. McDaid, S. Tyagi, E. Csizmadia, A. V. Graca-Souza, A. Liloia, M. P. Soares, L. E. Otterbein, A. Usheva, K. Yamashita, F. H. Bach, *Circulation* **2005**, *112*, 1030–1039; e) P. Keshavan, T. L. Deem, S. J. Schwemberger, G. F. Babcock, J. M. Cook-Mills, S. D. Zucker, *J. Immunol.* **2005**, *174*, 3709–3718.

[4] a) M. Alexandra Brito, R. F. Silva, D. Brites, *Clin. Chimica Acta* **2006**, *374*, 46–56; b) R. Brodersen, L. Stern, *Neuropediatrics* **1987**, *18*, 34–36; c) M. M. Thaler, *Nature New Biol.* **1971**, *230*, 218–219; d) J. F. Watchko, C. Tiribelli, *N. Engl. J. Med.* **2013**, *369*, 2021–2030.

[5] a) X. Q. Zhang, O. Even-Or, X. Xu, M. van Rosmalen, L. Lim, S. Gadde, O. C. Farokhzad, E. A. Fisher, *Adv. Healthcare Mater.* **2015**, *4*, 228–236; b) A. Meddahi-Pellé, A. Legrand, A. Marcellan, L. Louedec, D. Letourneur, L. Leibler, *Angew. Chem. Int. Ed.* **2014**, *53*, 6369–6373; *Angew. Chem.* **2014**, *126*, 6487–6491; c) L. Yin, Z. Song, Q. Qu, K. H. Kim, N. Zheng, C. Yao, I. Chaudhury, H. Tang, N. P. Gabrielson, F. M. Uckun, J. Cheng, *Angew. Chem. Int. Ed.* **2013**, *52*, 5757–5761; *Angew. Chem.* **2013**, *125*, 5869–5873; d) L. B. Vong, T. Tomita, T. Yoshitomi, H. Matsui, Y. Nagasaki, *Gastroenterology* **2012**, *143*, 1027–1036; e) C. K. Kim, T. Kim, I. Y. Choi, M. Soh, D. Kim, Y. J. Kim, H. Jang, H. S. Yang, J. Y. Kim, H. K. Park, S. P. Park, S. Park, T. Yu, B. W. Yoon, S. H. Lee, T. Hyeon, *Angew. Chem. Int. Ed.* **2012**, *51*, 11039–11043; *Angew. Chem.* **2012**, *124*, 11201–11205; f) S. Kannan, H. Dai, R. S. Navath, B. Balakrishnan, A. Jyoti, J. Janisse, R. Romero, R. M. Kannan, *Sci. Transl. Med.* **2012**, *4*, 130ra146.

[6] a) A. R. Kundur, I. Singh, A. C. Bulmer, *Atherosclerosis* **2015**, *239*, 73–84; b) S. Jangi, L. Otterbein, S. Robson, *Int. J. Biochem. Cell Biol.* **2013**, *45*, 2843–2851; c) R. Öllinger, H. Wang, K. Yamashita, B. Wegiel, M. Thomas, R. Margreiter, F. H. Bach, *Antioxid. Redox Signaling* **2007**, *9*, 2175–2185.

[7] S. E. Boiadjiev, K. Watters, S. Wolf, B. N. Lai, W. H. Welch, A. F. McDonagh, D. A. Lightner, *Biochemistry* **2004**, *43*, 15617–15632.

[8] a) C. Nathan, A. Cunningham-Bussel, *Nat. Rev. Immunol.* **2013**, *13*, 349–361; b) M. Mittal, M. R. Siddiqui, K. Tran, S. P. Reddy, A. B. Malik, *Antioxid. Redox Signaling* **2014**, *20*, 1126–1167.

[9] C. M. Steyers 3rd, F. J. Miller, Jr., *Int. J. Mol. Sci.* **2014**, *15*, 11324–11349.

[10] a) Y. Yan, V. Kolachala, G. Dalmasso, H. Nguyen, H. Laroui, S. V. Sitaraman, D. Merlin, *PloS ONE* **2009**, *4*, e6073; b) X. D. Li, Y. H. Chiu, A. S. Ismail, C. L. Behrendt, M. Wight-Carter, L. V. Hooper, Z. J. Chen, *Proc. Natl. Acad. Sci. USA* **2011**, *108*, 17390–17395.

[11] M. J. Maisels, A. F. McDonagh, *N. Engl. J. Med.* **2008**, *358*, 920–928.

Received: March 11, 2016
Revised: April 11, 2016
Published online: May 4, 2016

 © 2016 Wiley-VCH Verlag GmbH & Co. KGaA, Weinheim